Transmission Security for Single, Hair Follicle–Related Tactile Afferent Fibers and Their Target Cuneate Neurons in Cat

M. K. ZACHARIAH, G. T. COLEMAN, D. A. MAHNS, H. Q. ZHANG, AND M. J. ROWE
School of Physiology and Pharmacology, University of New South Wales, Sydney, NSW 2052, Australia

Received 23 February 2001; accepted in final form 17 April 2001

Zachariah, M. K., G. T. Coleman, D. A. Mahns, H. Q. Zhang, and M. J. Rowe. Transmission security for single, hair follicle–related tactile afferent fibers and their target cuneate neurons in cat. *J Neurophysiol* 86: 900–911, 2001. Transmission from single, identified hair follicle afferent (HFA) nerve fibers to their target neurons of the cuneate nucleus was examined in anesthetized cats by means of paired recording from individual cuneate neurons and from fine, intact fascicles of the lateral branch of the superficial radial nerve in which it is possible to identify and monitor the activity of each group II fiber. Selective activation of individual HFA fibers was achieved by means of focal vibrotactile skin stimulation. Forearm denervation precluded inputs from sources other than the monitored HFA sensory fiber. Transmission characteristics were analyzed for 21 HFA fiber-cuneate neuron pairs in which activity in the single HFA fiber of each pair reliably evoked spike output from the target neuron at a fixed latency. As the cuneate responses to each HFA impulse often consisted of 2 or 3 spikes, in particular at HFA input rates up to ~20 imp/s, the synaptic linkage displayed potent amplification and high-gain transmission, characteristics that were confirmed quantitatively in measures of *transmission security* and cuneate *spike output* measures. In response to vibrotactile stimuli, the tight phase locking in the responses of single HFA fibers was well retained in the cuneate responses for vibration frequencies up to ~200 Hz. On measures of *vector strength*, the phase locking declined across the synaptic linkage by no more than ~10% at frequencies up to 100 Hz. However, limitations on the impulse rates generated in both the HFA fibers their associated cuneate neurons meant that the impulse patterns could not directly signal information about the vibration frequency above 50–100 Hz. Although single HFA fibers are also known to have secure synaptic linkages with spinocervical tract neurons, it is probable that this linkage lacks the capacity of the HFA-cuneate synapse for conveying precise temporal information, in an impulse pattern code, about the frequency parameter of vibrotactile stimuli.

INTRODUCTION

Vibrotactile information from the glabrous skin of the limb extremities is derived largely from dynamically sensitive tactile afferent fibers associated with Pacinian corpuscle (PC) receptors and from intradermal encapsulated receptors that, in the cat, are known as Krause corpuscles. The two classes of afferent fibers in the cat are known, respectively, as PC fibers and *rapidly adapting* (RA) afferent fibers (Ferrington and Rowe 1980a; Ferrington et al. 1984; Iggo and Ogawa 1977; Jänig 1971; Jänig et al. 1968). In the hairy skin, the principal tactile afferent fibers responsible for vibrotactile detection appear to be associated with hair follicles of the *guard hair* type (Burgess et al. 1968; Merzenich and Harrington 1969) as PC afferent fibers are rare or absent in hairy skin (Brown and Iggo 1967; Tuckett et al. 1978). The *hair follicle afferent* (HFA) fibers are purely dynamically sensitive and therefore display rapidly adapting responses to static skin displacement. In response to vibrotactile stimuli they may respond to frequencies up to 200–300 Hz but have substantially higher thresholds than their glabrous skin counterparts (Merzenich and Harrington 1969; Tuckett et al. 1978). On the assumption that human HFA fibers have similar thresholds to those in the cat, these regional differences among tactile afferents from glabrous and hairy skin may account, at least in part, for the higher subjective thresholds for human vibrotactile sensation in hairy skin (Merzenich and Harrington 1969; Verrillo 1966) compared with those in glabrous skin (Talbot et al. 1968).

However, whether the transmission characteristics across synaptic junctions in the central tactile pathways also limit the capacity of HFA fibers to contribute to subjective vibrotactile perceptual performance is uncertain. While single HFA fibers are known to exert potent synaptic actions on dorsal horn neurons that give rise to the spinocervical tract (Brown et al. 1987a–c), it is not known whether they display a similar high security in their synaptic linkage with target neurons of the dorsal column nuclei in the principal tactile sensory pathway. The broad aims of the present study were to examine the transmission characteristics for the synaptic linkage formed between single HFA fibers and their target neurons of the cuneate nucleus. Specific aims were to determine first whether input from a single HFA fiber is sufficient to activate central target neurons and therefore reveal whether the transmission of vibrotactile information derived from individual HFA fibers can take place without spatial summation; second, whether temporal summation is necessary for the effective transmission of single HFA inputs to the cuneate neurons, and third, whether vibrotactile frequency information, encoded in the phaselocked impulse patterns of single HFA fibers, can be reliably retained in a temporal patterning code in the course of transmission across the cuneate synaptic linkage.

The analysis of transmission efficacy in the one-to-one linkage was based on a simultaneous, paired recording paradigm of the type used in our earlier studies of transmission security for PC and *slowly adapting* tactile afferent fibers (Ferrington et al. 1987a,b; Gynther et al. 1995; Vickery et al. 1994). In the present study the simultaneous paired recordings were made

Address reprint requests to M. J. Rowe (E-mail: M.Rowe@unsw.edu.au).

The costs of publication of this article were defrayed in part by the payment of page charges. The article must therefore be hereby marked "*advertisement*" in accordance with 18 U.S.C. Section 1734 solely to indicate this fact.

from an individual HFA fiber in an intact fascicle of the lateral branch of the superficial radial nerve, and from a cuneate target neuron of that identified HFA fiber. Preliminary reports of this work have been presented in conference proceedings (Zachariah et al. 1999a,b).

METHODS

Animal preparation and stimulation procedures

Data were obtained in experiments performed on adult cats in which anesthesia was induced and maintained with sodium pentobarbitone (40 mg/kg ip; <2 mg $\cdot$ kg^{-1} $\cdot$ h^{-1} iv; overdose at end of experiment). All experiments conformed with the Australian Code of Practice for the Care and Use of Animals for Scientific Purposes. The trachea was cannulated, as were the femoral artery and vein for the continuous monitoring of blood pressure and heart rate, and for infusion of anesthetic agent and fluids. Temperature was maintained at 38 $\pm$ 0.5°C. An extensive denervation of the forearm was performed by sectioning the ulnar, median, median cutaneous, and musculocutaneous nerves to preclude inputs arising from sources other than the nerve fascicles under study.

The lateral branch of the superficial radial nerve (LB-SRN) was exposed distal to the elbow and maintained under paraffin oil. In each experiment, longitudinal dissection of the nerve into approximately 10 fascicles was carried out over distances of 3–5 cm by opening the epineurial sheath, freeing individual fascicles from surrounding connective tissue within the overall nerve, and longitudinally dividing certain of the larger fascicles. The fascicles were initially kept in continuity with the CNS, to permit recording from individual fascicles by means of a platinum hook electrode. The innervation field of each could then be identified by manual stimulation of the dorsal surface of the forearm. Most fascicles were then sectioned leaving just three to five of them intact.

The skin in the field of superficial radial innervation on the dorsum of the paw and the distal forelimb was shaved to allow accurate positioning of the stimulator probe on hair follicles or at the root of the hairs for effective stimulation of individual HFA fibers. The receptive fields of individual fibers within the fascicles were carefully mapped using low strength von Frey hairs (~0.02–0.2 g wt). Three to five fascicles with identified and discrete innervation fields on the paw dorsum were usually selected, and other fascicles, including those that innervated the wrist or proximal forelimb or that had high spontaneous activity, were sectioned, as was the medial branch of the superficial radial nerve. Individual HFA fibers were selectively activated by applying precisely controlled vibrotactile stimuli to their receptive fields on the skin (Fig. 1) using a fine stimulus probe (0.25 mm diam) driven by a feedback-controlled mechanical stimulator (Ferrington et al. 1987a,b; Vickery et al. 1994; Zhang et al. 1996).

The dorsal column nuclei (DCN) were exposed by removing small parts of the atlas and occiput. Single cuneate neurons, in the region between 1 and 4 mm caudal to the obex, that received input from an identified HFA fiber were located and recorded extracellularly by means of tungsten microelectrodes. When a cuneate neuron was activated by hair inputs from the dorsum of the distal forelimb, its receptive field was mapped with the aid of a dissecting microscope and von Frey hairs, and paired simultaneous recordings were then made from the neuron and from individual HFA fibers that exerted suprathreshold excitatory actions on this cuneate neuron. Selective activation of individual HFA fibers was achieved by means of focal tactile stimuli delivered to the skin at the point of maximum sensitivity for the HFA fiber, with the 0.25-mm-diam flat-tipped probe, usually oriented perpendicular to the skin surface and placed, in the resting position, fractionally above it (~100 μm). Vibrotactile stimuli were delivered in 1-s-long trains with the sinusoidal vibration superimposed on a 1.5-s background step indentation of 400 μm, and commenced 300 ms after the onset of the step (Fig. 1, *inset*). Stimulus repetition rate was usually 1 per 8–10 s to allow recovery of skin position.

Recording and analysis procedures

Impulse activity recorded from the afferent fiber-cuneate neuron pair was stored on magnetic tape and in a laboratory computer.

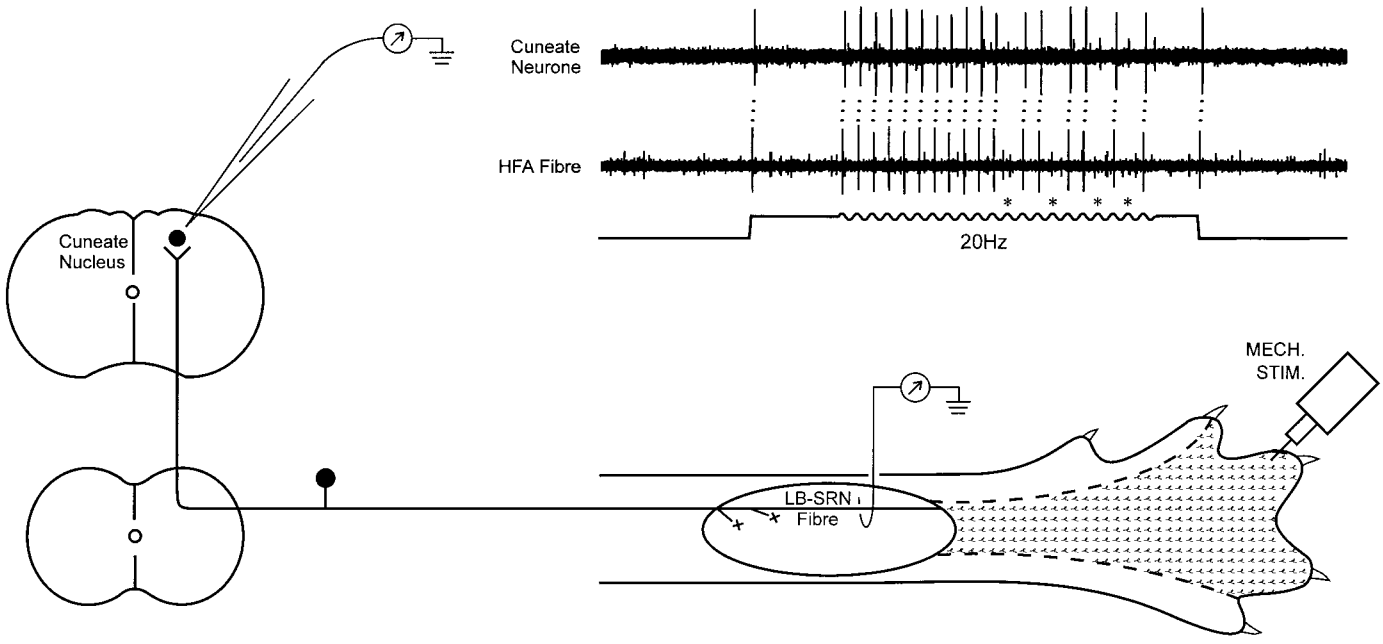

FIG. 1. Schematic representation of the experimental arrangement for paired, simultaneous recording from single, hair follicle afferent (HFA) fibers and their target cuneate neurons. Impulse traces in the *inset* show the simultaneously recorded responses of an HFA fiber–cuneate neuron pair to a 1-s train of 20-Hz cutaneous vibration superimposed on a background steady indentation as represented by the waveform beneath the impulse traces (*top impulse trace*, cuneate neuron; *bottom impulse trace*, HFA fiber in Fig. 1 and other figures). Asterisks indicate those cycles of vibration where the HFA fiber failed to respond, and there was a correlated failure of the target neuron to respond. LB-SRN, lateral branch of the superficial radial nerve.

Impulse rates (in imp/s) were obtained in response to the 1-s vibration trains to plot stimulus-response relations for the HFA fiber-cuneate neuron pairs. Transmission characteristics for the pair were also quantified with two further measures, the *transmission security*, and a cuneate *spike output* measure. The first, transmission security, was defined as the proportion of HFA impulses that evoked a response in the cuneate neuron. This spike output measure was calculated from latency histograms (LHs) (Vickery et al. 1994), which are modified cross-correlograms constructed from impulse activity elicited in the cuneate neuron in response to HFA fiber impulses, by treating successively each HFA fiber impulse as *time 0*. The LHs permitted accurate determination of the latency to the onset of the central neuron response, as well as the transmission security measure. The second measure, of cuneate spike output to successive HFA input spikes, was obtained when the HFA input fiber was responding (at least in the early segment of the vibration train) at or near a regular 1:1 impulse level; that is, with one impulse discharging on each cycle of the vibration. This spike output measure was computed as a mean from usually five successive response sequences for a given vibration stimulus.

Evaluation of temporal patterning in HFA-cuneate paired responses to vibration

The analysis of temporal patterning in the vibrotactile responses was based on construction of peristimulus time histograms (PSTHs) and cycle histograms from which quantitative measures of phase locking could be obtained (Ferrington et al. 1987a,b; Mackie et al. 1998, 1999; Vickery et al. 1994). The cycle histograms use a pulse associated with the onset of each successive cycle in a vibration train as a stimulus marker and display the incidence of impulse occurrences at different times throughout the period of the vibration cycle. Two measures of phase locking were obtained, the *percentage entrainment* and the *resultant*. Percentage entrainment corresponded to the maximum percentage of total impulse occurrences that falls within any continuous half cycle of the vibration cycle period and could range from a minimum of 50%, characteristic of a rectangular distribution in the cycle histogram and an absence of phase locking, to a maximum of 100%. The resultant (R) was derived from the cycle histogram distributions as a measure of *vector strength* in the cyclic distribution. This measure is based on directional or angular statistics (Mardia 1972) and quantifies the phase coherence or synchronization in the impulse distribution. This measure has been used in evaluating the entrainment of auditory responses to tonal stimuli (e.g., Bledsoe et al. 1982; Lavine 1971) and in the somatosensory system for quantifying the entrainment of responses to vibrotactile stimuli (Greenstein et al. 1987; Mackie et al. 1998; Vickery et al. 1994). The resultant, *R*, was calculated from each cycle histogram distribution according to the formula

$$R = \sqrt{\{[\Sigma \cos (x_i)/n]^2 + [\Sigma \sin (x_i)/n]^2\}}$$

where n is the total number of impulse occurrences, and $x_i(1 \rightarrow n)$ is the phase angle (in radians) of each spike occurrence time relative to the start of the vibration cycle (Zar 1984). The resultant can provide a more sensitive measure of phase locking than percentage entrainment in cases in which all spike activity is confined within one half-cycle of the vibration waveform. In this circumstance the percentage entrainment is always 100% whether the spikes are distributed throughout the half cycle or confined to a limited segment of it.

RESULTS

Input to cuneate neurons from single HFA fibers

The innervation field on the dorsal surface of the forearm was mapped for each of the fascicles of the LB-SRN that had been separated by longitudinal division of the nerve. This was carried out by recording from each fascicle in turn with a platinum hook electrode while manually stimulating the skin with a fine brush or von Frey hair. Most fascicles were then sectioned leaving usually three, but up to five, in continuity with the CNS. Fascicles that were selected to remain intact were chosen according to the following criteria. First, the fascicle needed to be sufficiently fine that the signal-to-noise ratio (usually 5–10:1) for single fiber responses ensured a clear discontinuity between the recorded signals and background noise levels (see Figs. 1, 2, and 4). Second, low levels of spontaneous activity were required to permit clear isolation of activity from the identified HFA fiber under study. Third, each of the selected fascicles had a discrete field of innervation, on the forearm, precluding the risk of contaminating inputs being generated over fascicles other than the one being monitored. Other nerves to the forearm were sectioned, including those that have some overlap with the innervation field of the LB-SRN, such as the medial branch of superficial radial and the ulnar nerve. We can therefore be quite confident in our assumption that, in the paired recording analysis, the monitored HFA fiber was the only one responsible for the observed cuneate responses.

Location of cuneate neurons activated by single HFA fibers

Transmission characteristics were examined for 21 HFA fiber-cuneate neuron pairs in which activity in single, identified HFA fibers reliably evoked spike output from the target neuron (e.g., Fig. 1, *inset*). The cuneate neurons were identified by microelectrode tracking in the region of distal forelimb representation of the nucleus while lightly brushing the skin in the innervation zones of the selected, surviving fascicles of the LR-SRN. All but 2 of the 21 recorded cuneate neurons were located between 1 and 3 mm caudal to the obex, at a mediolateral position between 1 and 2 mm lateral to the midline, and at depths below the brain stem surface of 0.5–3 mm. The two neurons outside these locations included one found 0.5 mm caudal to the obex and one at 0.8 mm lateral to the midline. These locations were therefore consistent with the neurons being in the cluster zone of the cuneate nucleus (Hand and Van Winkle 1977), where almost all neurons sampled with the extracellular recording technique are known to be thalamocortical projection neurons (Andersen et al. 1964; Brown et al. 1974; Gordon and Jukes 1964).

Capacity of single HFA fibers to drive cuneate neurons

Our interpretation that the monitored HFA fiber was uniquely responsible for the associated cuneate neuron responses in circumstances such as the Figs. 1 and 2 traces, is based, as indicated above, on the denervation procedures and the stated signal-to-noise recording requirements. However, in addition, it is apparent in these figures that the cuneate neuron responses were dependent on the prior occurrence of the observed HFA fiber spike and followed at a consistent latency. Furthermore, when the HFA fiber failed to respond on some cycles of the vibrotactile stimulus in the impulse traces of Figs. 1 and 2, there was a correlated failure of response in the cuneate neuron. This is indicated by the asterisks in Fig. 1 and occurs in Fig. 2 on many of the 20-Hz vibration cycles at the

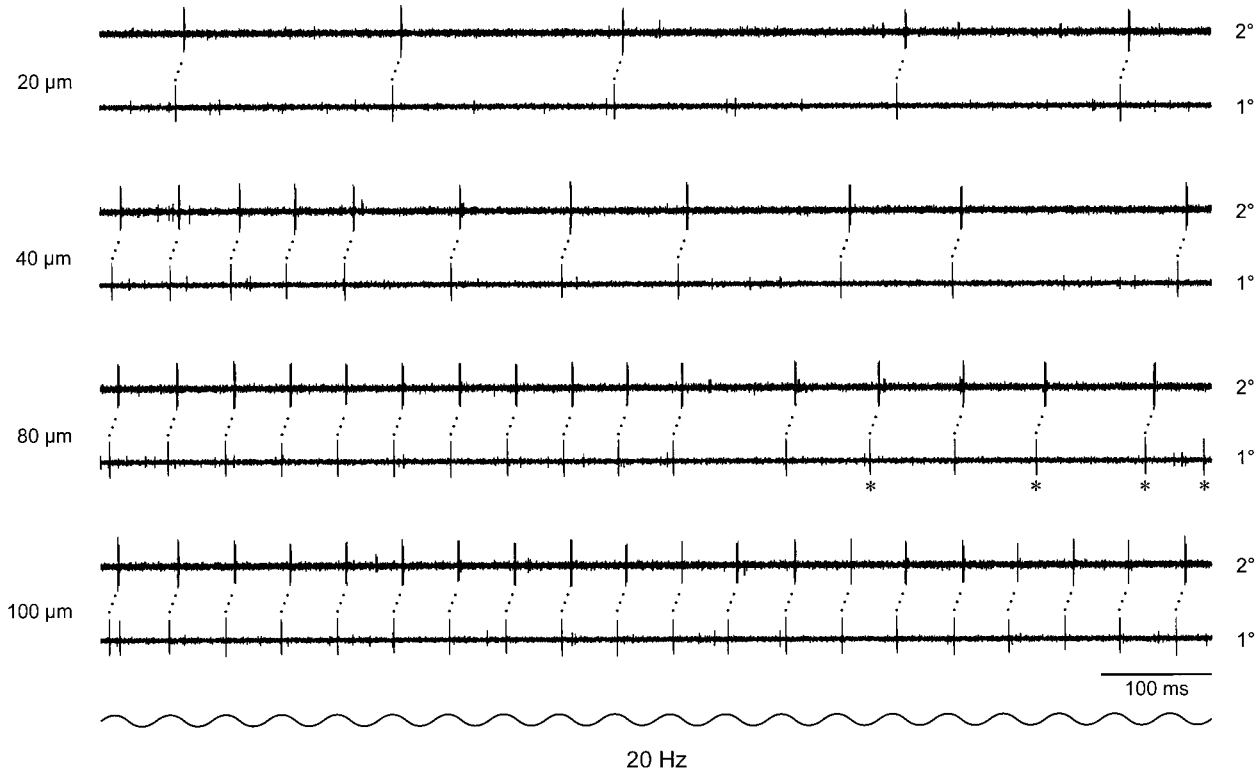

FIG. 2. The capacity of individual HFA fiber spikes to generate spike output from a cuneate target neuron. Paired recording traces were obtained in response to vibrotactile stimulation at 20 Hz delivered to dorsal surface of the paw. The high security of the linkage for the pair is revealed by the presence of the cuneate neuron spikes (designated 2° in *top trace*) in response to almost every HFA fiber spike (designated 1° in *bottom trace*) for each of the 4 amplitudes of the vibration stimulus (20–100 μm). The *bottom trace* shows the 1-s long train of vibration at 20 Hz.

low amplitudes (20 and 40 μm) and on two of the cycles at the 80-μm amplitude. Further strong evidence for the dependence of the cuneate spikes on the monitored HFA fiber spikes may be seen in the 80-μm paired traces in Fig. 2 when the HFA fiber displayed an unusual jump to a different phase relation with the vibration waveform on cycles 14, 17, 19, and 20 (as indicated by the asterisks). The related cuneate neuron response shows a corresponding shift in its phase relation.

The reliable correlation between the HFA spikes and the paired cuneate responses is apparent from the connecting dot sequence in the impulse traces of Figs. 1 and 2. The latency for the cuneate responses, measured as the delay between the time of occurrence of the HFA spike at the forearm recording site and the cuneate response ranged from 4.1 to 7.8 ms with a mean latency of 5.39 $\pm$ 1.25 ms (mean $\pm$ SD, $n = 20$). This time corresponds to the conduction time plus the time for synaptic transmission. If 1 ms is allowed for the central synaptic delay time in the cuneate nucleus, one obtains an average conduction velocity estimate of ~57 m/s, based on a conduction distance of ~25 cm. This value is consistent with HFA fibers falling in the group II range of afferent conduction velocities even though the estimate includes both peripheral and the somewhat slower central conduction components (Brown 1968). The latency histograms (see METHODS) in Fig. 3 show the reliable, fixed latency of cuneate responses for two HFA fiber-cuneate neuron pairs and were constructed in both *A* and *B* from the cuneate responses to ~200 input spikes in the HFA fiber's response to vibration (20 Hz in *A*, and 30 Hz in *B*). The paired impulse traces show that the double or multiple peaks in the latency histograms are attributable to pairs or bursts of spikes discharged by the cuneate neuron and do not reflect alternative preferred phases of response for the cuneate neuron. The initial spike in the cuneate response occurs with a fixed latency and shows less temporal jitter than the second or third spike in the cuneate response.

Despite the close temporal correlation between the paired peripheral and central responses, it was clear that the latter were not obtained from the central axon of the peripherally recorded HFA fiber as they often consisted of pairs or a burst of spikes and therefore did not match the peripheral activity. In addition, at higher rates of HFA fiber activity, the central response did not follow every occurrence of the HFA spike, reflecting a breakdown of security for the synaptic linkage. Furthermore, the central spikes had the di- or tri-phasic configuration and duration $\geq$0.5 ms that is consistent with extracellular microelectrode recording from the soma rather than an axon (Winter 1965).

Security of the synaptic linkage for HFA fiber-cuneate neuron pairs

Some variation was observed in the security of the linkage among the 21 HFA fiber-cuneate neuron pairs studied, although *all* 21 demonstrated the capacity of individual HFA fibers to exert suprathreshold excitatory actions on cuneate target neurons. Furthermore, as these actions entailed a single HFA spike generating spike output from the cuneate target neuron, it is clear that each of these HFA fibers generated

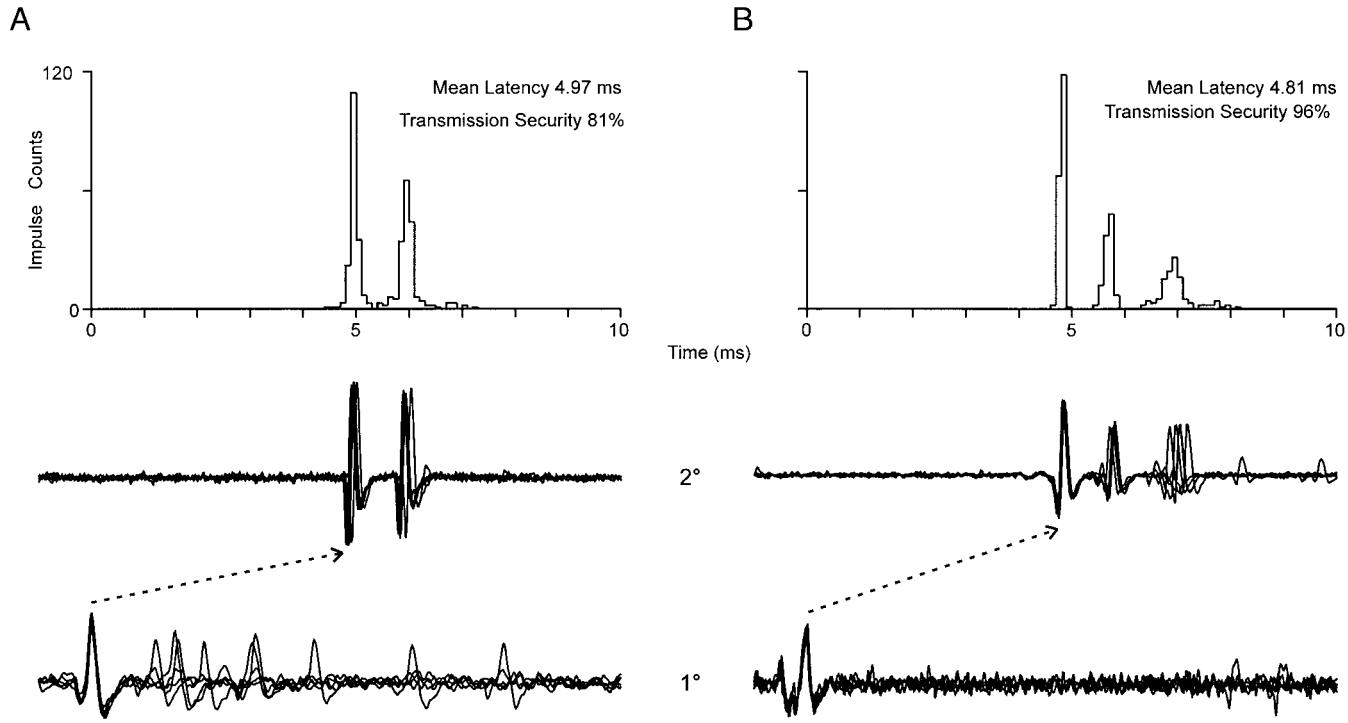

FIG. 3. Amplified responses of cuneate neurons to single impulses in identified HFA fibers. Latency histograms, constructed from the responses to skin vibration of 2 HFA fiber–cuneate neuron pairs, are plotted in the *top sections* of *A* and *B*. The histograms of the accumulated cuneate responses indicate the time of occurrence of action potentials in the target cuneate neurons following the HFA fiber impulses (*time 0*). The responses in the 2 cuneate neurons occurred at a consistent onset latency, of 5 and 4.8 ms, respectively, in *A* and *B*. The multiple peaks in these histograms demonstrate the tendency of the cuneate neuron to respond to a single input spike with a burst of action potentials, and at a consistent short latency. The expanded waveforms of the target cuneate neuron spikes and those of the associated HFA fiber are shown, respectively, in the *bottom segments* of the figure.

unitary excitatory postsynaptic potentials (EPSPs) that exceeded threshold for spike discharge in the cuneate neuron. The high security of the synaptic linkage for many of the pairs was demonstrated by the presence of a cuneate neuron spike response to all or almost all of HFA spikes (Figs. 1 and 2). In Fig. 2, this capacity of the HFA fiber (1° in *bottom trace* of each pair) to securely drive the target neuron (2° in *top trace*) was sustained over the 1-s duration of the vibrotactile stimulus train as the discharge rate in the HFA fiber progressively increased as a function of vibration amplitude (from 20 to 100 μm) to a plateau level of 1 impulse per cycle of the 20-Hz vibration. At this 1:1 level of response, the HFA fiber unfailingly generated spike output in the cuneate neuron as indicated by the linking dotted lines in the lowest set of paired traces (100 μm) in Fig. 2.

Amplification of input in the HFA-cuneate neuron synaptic linkage

At the level of peripheral drive (20 imp/s) illustrated in Fig. 2, the majority of HFA spikes gave rise to a pair of spikes in the target neuron. Although not easily visualized at the illustrated time scale of the traces in Fig. 2, this was the case for each of the 1st 10 cycles of the 20-Hz input in the 100-μm trace and for ½ the remaining 10 cycles. However, the capacity for amplification of the input signal across the one-to-one HFA-cuneate linkage is clearer in the data shown for the two pairs illustrated in Fig. 3 and for the paired data in Fig. 4. This form of amplification of the input signal across the 1:1 synaptic linkage was apparent for half (10 of 21) of the HFA fiber-cuneate neuron pairs analyzed and consisted of a pair (Fig. 3*A*) or burst of spikes (Fig. 3*B*) in response to the single incoming HFA spike. In Fig. 4, a burst of three spikes was discharged by the cuneate neuron in response to the initial HFA spike in the incoming train at 20, 50, and 100 Hz, and an amplified response, in the form of a spike doublet, was sustained for subsequent HFA spikes in the 10-cycle segments shown in Fig. 4 at 20 and 50 Hz. However, the capacity of the linkage to sustain this amplification declined at higher rates of peripheral drive as illustrated in the lowest paired traces in Fig. 4 where the HFA fiber was driven at a rate of 100 imp/s by a 100-Hz vibrotactile stimulus. Nevertheless, each HFA spike activated on the 1st 8 cycles of the 100-Hz vibration stimulus elicits a reliable single spike output from the cuneate neuron.

For many pairs, the amplification of input signal was sustained over the vibrotactile response range of the HFA fiber, in particular, when the fibers were restricted in their vibrotactile responsiveness to impulse rates of $<$50 imp/s. The four stimulus-response relations of Fig. 5 show this amplification for one pair when the HFA fiber was activated by 20-, 50-, 80-, and 100-Hz vibration stimuli. The HFA fiber displayed a 1:1 response plateau of $\sim$20 imp/s in response to the 20-Hz vibration and at other vibration frequencies attained a maximum impulse rate of 30–35 imp/s. However, at all levels of response in the presynaptic element, the cuneate neuron output was amplified reflecting the high-gain transmission for the HFA-cuneate synaptic linkage.

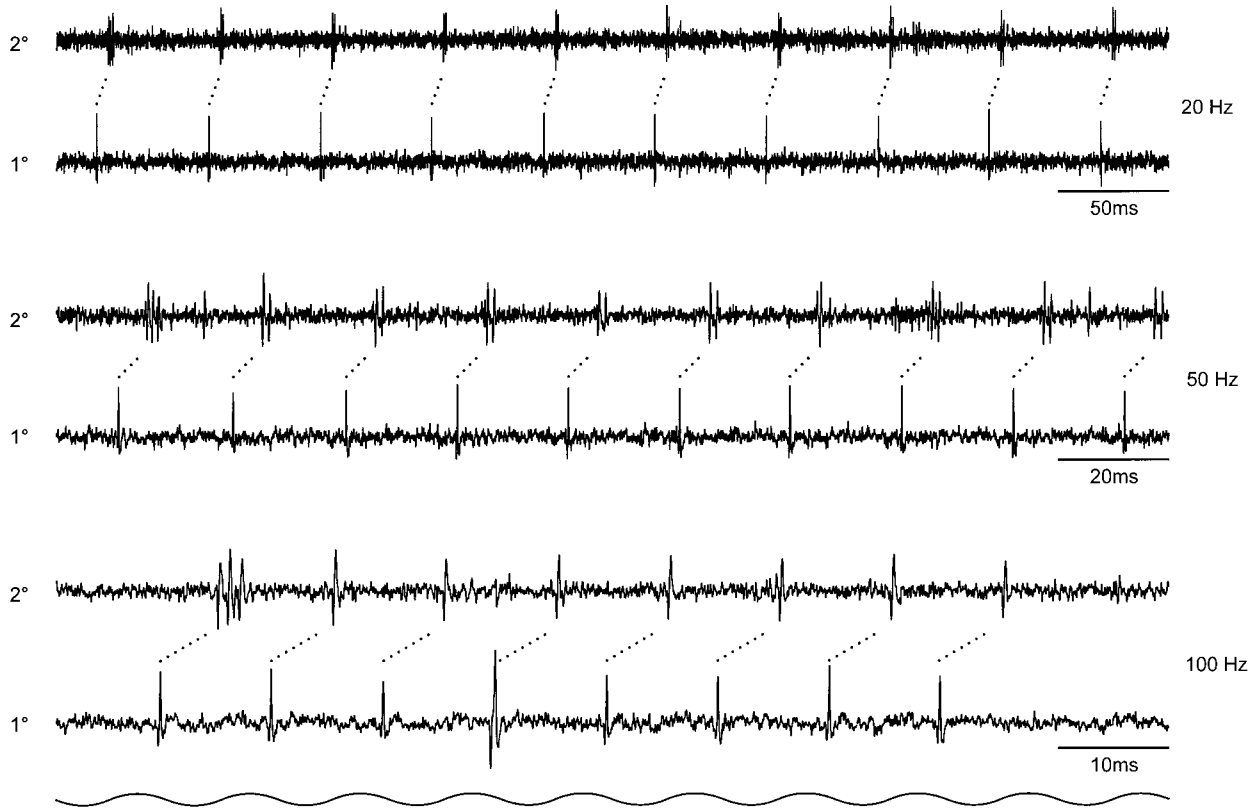

FIG. 4. The capacity of the one-to-one cuneate synaptic linkage to amplify individual HFA fiber signals as a function of different impulse rates in the HFA input. In each set of impulse traces, the *top trace* (2°) shows the responses of the cuneate neuron to different HFA fiber spike trains, represented in the *bottom impulse trace* (1°). Responses of the HFA fiber–cuneate neuron pair to 20-, 50-, and 100-Hz sinusoidal vibration are shown in each set for the 1st 10 cycles at each frequency. While a single impulse in the primary HFA fiber produces a doublet response in the cuneate neuron at 20 and 50 Hz, this amplification is not sustained at the higher rate of input signal generated at 100 Hz.

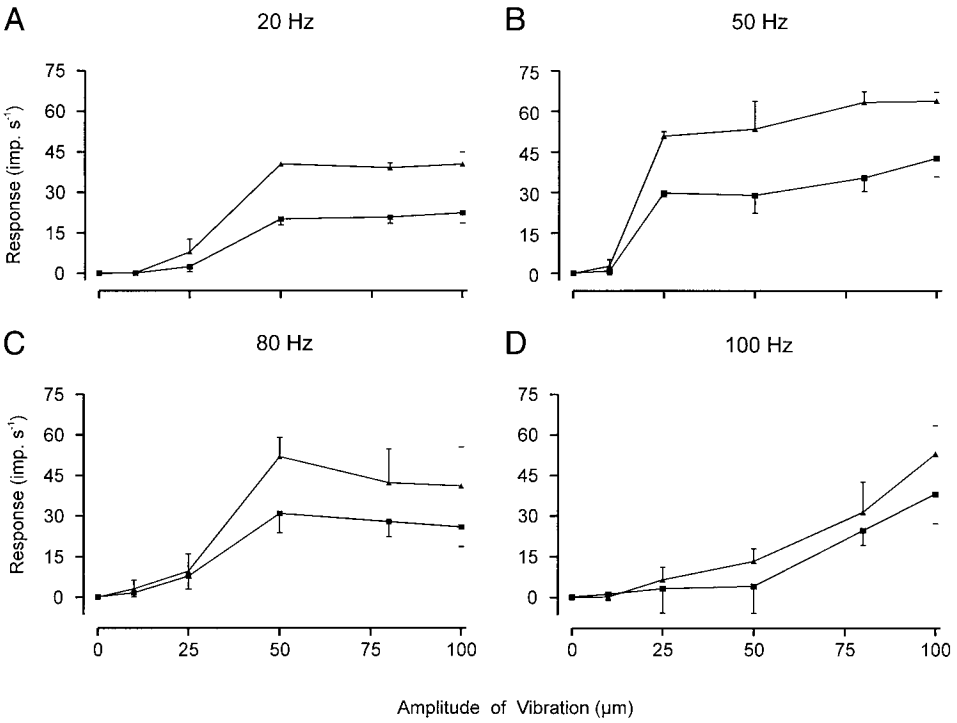

FIG. 5. Stimulus-response relations for vibration-induced responses of an HFA fiber–cuneate neuron pair. The graphs, constructed from responses to skin vibration lasting 1 s at 20, 50, 80, and 100 Hz, plot the mean response level (imp/s ± SD) against vibration amplitude from 10 repetitions of the stimulus. The HFA fiber data are plotted as filled squares and the target cuneate neuron data as filled triangles. The response level of both the HFA fiber and the cuneate neuron increases rather abruptly as a function of vibration amplitude and reveals some amplification of the presynaptic signal at most points across the stimulus-response range.

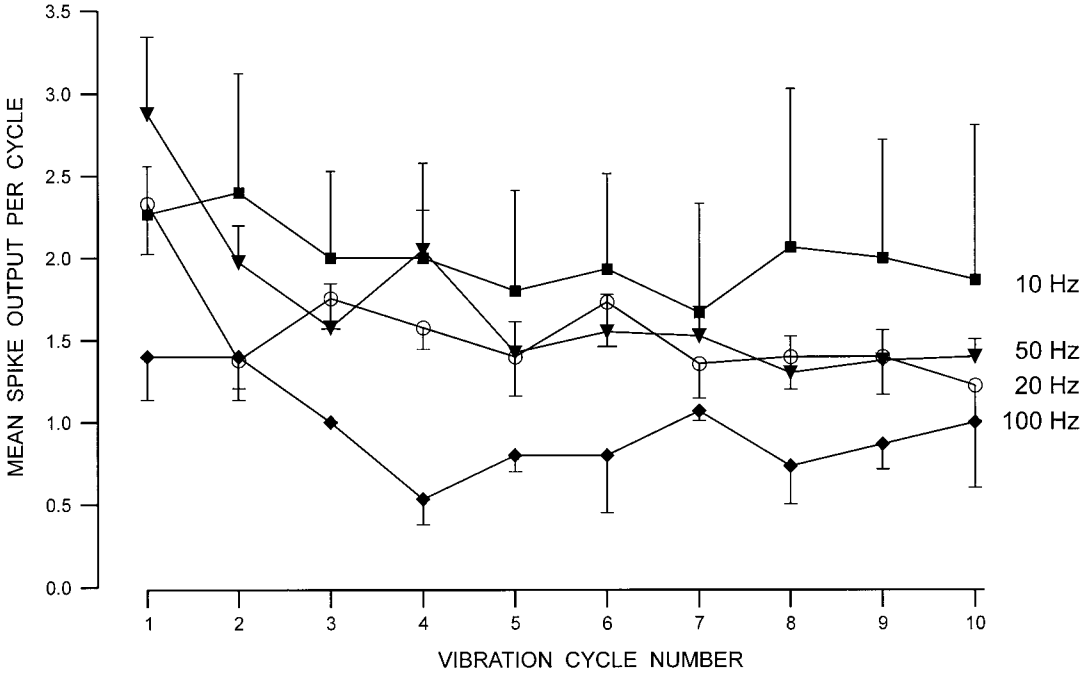

FIG. 6. Security of the linkage for HFA fiber–cuneate neuron pairs quantified as the averaged cuneate neuron spike output. The measure of the target cuneate neuron output was obtained for each pair when the HFA fiber was responding at 4 vibration frequencies with a regular 1:1 pattern of activity over these 1st 10 cycles of the vibration train. The mean spike output on each cycle (±SE; $n = 5$) was calculated and plotted for 9 pairs at 20 Hz, 8 pairs at 50 Hz, and for 3 pairs at each of 10 and 100 Hz. The graph shows that the synapse has the capacity to amplify input signals (i.e., generate cuneate output at >1 spike per cycle) even up to rates of input of ~50 imp/s; however, at the highest levels of peripheral drive (~100 imp/s) the amplification cannot be sustained although the synaptic security still remains remarkably high (cuneate spike output between 0.5 and 1 spike per cycle).

Quantification of transmission characteristics for HFA-cuneate neuron pairs

The transmission characteristics for HFA-cuneate pairs was quantified in two ways (see METHODS). The first measure, the transmission security, obtained from the latency histogram distributions (Fig. 3), was defined as the proportion of HFA fiber impulses that generated a response (1 or more impulses) in the cuneate neuron. In most pairs whose records are illustrated in Figs. 1, 2, 4, and 5, the transmission security was at or near 100%, while in Fig. 3, *A* and *B*, the values were 81 and 96%, respectively. For six pairs, in which the HFA fiber could be activated by 20- or 30-Hz vibration to discharge, with a regular 1:1 pattern of response over the full 1 s of the vibration train, the mean (±SD) transmission security was 90 ± 13% ($n = 6$). This value is similar to those obtained previously for the linkage between individual SAI or SAII fibers and their target cuneate neurons (Gynther et al. 1995; Vickery et al. 1994). However, at higher vibration frequencies (≥50 Hz), it was not possible to obtain reliable pooled transmission security measures, as there were too few HFA fibers that could be reliably driven with a regular 1:1 pattern of response to vibration over the full 1-s stimulus train.

A second quantitative measure of the transmission characteristics, the spike output from the cuneate neuron in response to successive HFA input spikes, is plotted in Fig. 6 as a function of vibration cycle number (or, in effect, input spike number, as the HFA fiber was responding at a 1:1 level over this early segment of the vibration train). For these four vibration frequencies, 10, 20, 50, and 100 Hz, the mean spike output for the cuneate neurons sampled was highest in response to the first and second incoming HFA spikes where the values were ~1.5–3.0 but remained high (>1.5) throughout the first 10 cycles at 10–50 Hz, reflecting the potent capacity for amplification in the linkage. However, at the 100-Hz level of drive, the amplification was not sustained beyond the first two HFA spikes, and mean spike output fell to levels between 0.5 and 1.0 spikes per cycle. The different mean spike output levels to the first spike (vibration cycle 1 on the abscissa) at the four frequencies reflect the different sample sizes and lack of identity in sampled pairs for the four vibration frequencies. The sample sizes were 3 at 10 Hz, 9 at 20 Hz, 8 at 50 Hz, and 3 at 100 Hz.

Although there was an initial decrement in the response output from the cuneate neuron over the first few cycles of the vibration (Fig. 6), the PSTHs on the *left* in Fig. 7, constructed over the full 1-s duration of the vibration train, show that cuneate responsiveness is then well maintained over the whole 1-s segment. Furthermore, part of the initial response decrement at the highest vibration frequency, 200 Hz, is attributable to a decline in the capacity of the HFA fiber to sustain its response to high-frequency vibration rather than a failure of the synaptic linkage.

Retention of phase locking and temporal patterning in responses to vibrotactile stimuli across the synaptic linkage between single HFA fibers and cuneate neurons

The expanded time scale for the PSTHs on the right-hand side in Fig. 7 shows the distribution of impulse occurrences over the 1st 30 cycles of vibration (at 30–200 Hz) for the cuneate neuron (*top histogram* of the pair) and the HFA fiber (*bottom histogram*). In both pre- and postsynaptic elements the

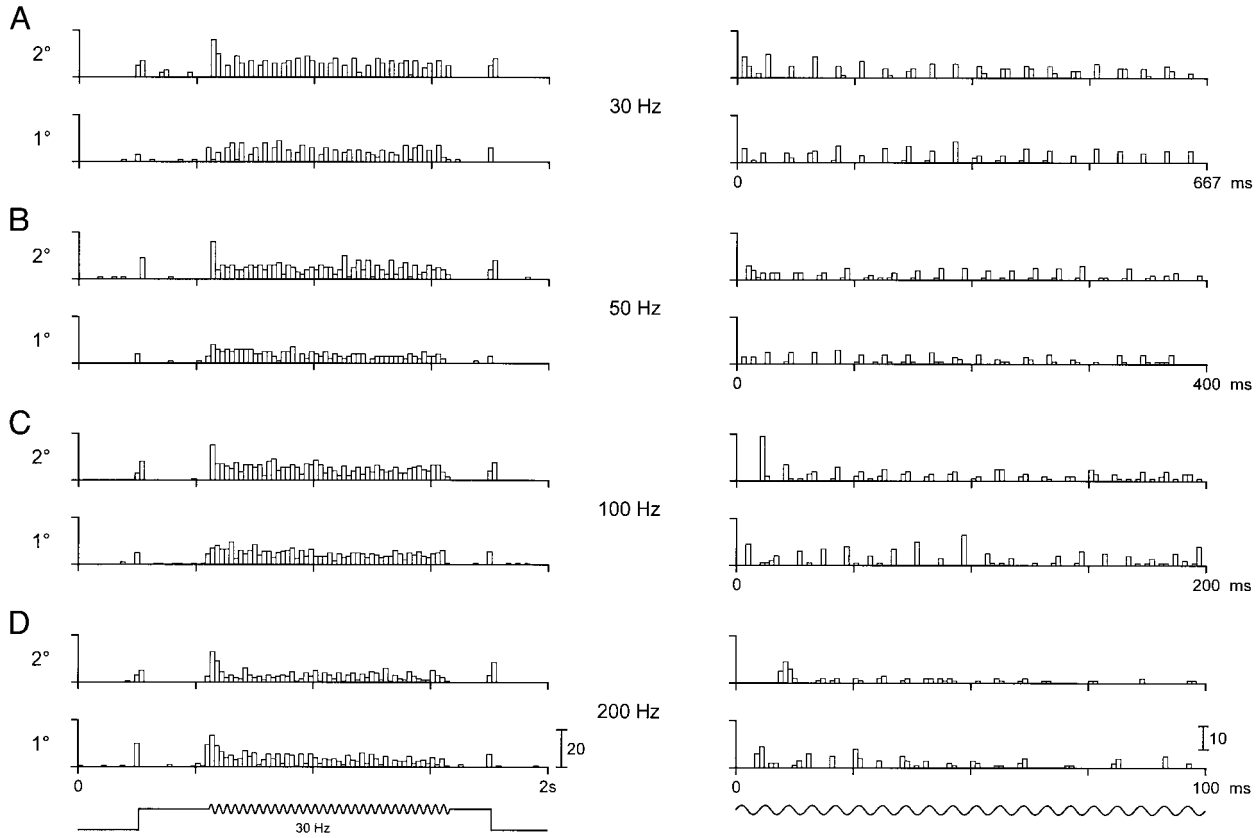

FIG. 7. Peristimulus time histograms (PSTHs) constructed from the responses of a target cuneate neuron and its associated HFA fiber. The pair of PSTHs making up each set (*A–D*) on the *left-hand side* show response profiles for the cuneate neuron (*top histogram* of each pair) and the HFA fiber (*bottom histogram* of each pair) to 1-s trains of vibration at 4 frequencies (from 30 to 200 Hz in *A–D*) superimposed on a 1.5-s steady indentation (stimulus waveform shown below). The height of each 50-ms column represents the number of impulse counts accumulated in each address. On the *right-hand side* the PSTH pairs have been expanded in time to show the phase locking in the responses during the 1st 30 cycles of vibration at each of the 4 frequencies (vertical calibration bars on *right-hand side* in *D* indicate the scale for accumulated impulse counts).

responses are phase locked as reflected in the preferential grouping of impulses at intervals approximating the cycle period, in particular at 30, 50, and 100 Hz. At 200 Hz there is only a weak response from the cuneate neuron, but the fiber itself is only weakly activated, although it displays some preferential grouping of spikes in the first 50 ms of the vibration train. In the responses to the 30, 50, and 100 Hz stimuli, the phase locking appears little if at all degraded in the cuneate neuron response compared with that of the HFA fiber. However, quantitative comparison of the tightness of phase locking in the pre- and postsynaptic elements was undertaken by constructing paired cycle histograms, as illustrated in Fig. 8, *A* and *B*, from the responses of two representative HFA-cuneate pairs to vibrotactile stimulation at four frequencies (20–200 Hz in *A*, and 30–200 Hz in *B*). In both pairs the responses display tight phase locking in both the pre- and postsynaptic elements. In *A*, the HFA responses at 20 and 50 Hz are confined within about one-quarter of the cycle period and spread to about one-third at 100 Hz and one-half at 200 Hz, with percentage entrainment values of ~100% at all four frequencies and *R* values of >0.9 except at 200 Hz, where there is greater spread of impulse occurrences and an *R* value of 0.83. The target cuneate neuron showed a very similar tight phase locking in its response, although percentage entrainment and *R* values were slightly lower on account of some scattered spike occurrences reflecting a low level of spontaneous activity that was unrelated to the vibration-induced response. For the second pair in *B*, there was no quantitative difference in the phase locking of pre- and postsynaptic elements except for the slightly greater dispersion in the cuneate neuron responses at the highest frequency, 200 Hz, where the *R* value was 0.73 compared with 0.85 for the HFA fiber.

For six pairs that were studied at a series of frequencies, the quantitative measures of phase locking based on the *R* values are plotted as a function of vibration frequency in Fig. 9. The data for each linked pair in *A* and *B* show that, for all six, the cuneate neuron displays little decline in the phase locking of its responses compared with its HFA input fiber. On average the decline in *R* values over the vibration frequency range up to 100 Hz was <10% (from ~0.85 to ~0.8), although at the higher frequency of 200 Hz the central neurons showed a more marked decline, to an *R* value of ~0.45 compared with ~0.7 in the HFA fibers. Comparison of the peripheral *R* values with those of their central target neurons in Fig. 9*C*, using an ANOVA, confirmed that the small decline in the tightness of phase locking across this one-to-one synaptic linkage was significant (F ratio 4.08; $P < 0.05$). Furthermore, comparison, with a paired t-test, of the pooled peripheral *R* values in Fig. 9*C* with the pooled cuneate values, also confirmed the significant difference between the two samples ($P < 0.001$).

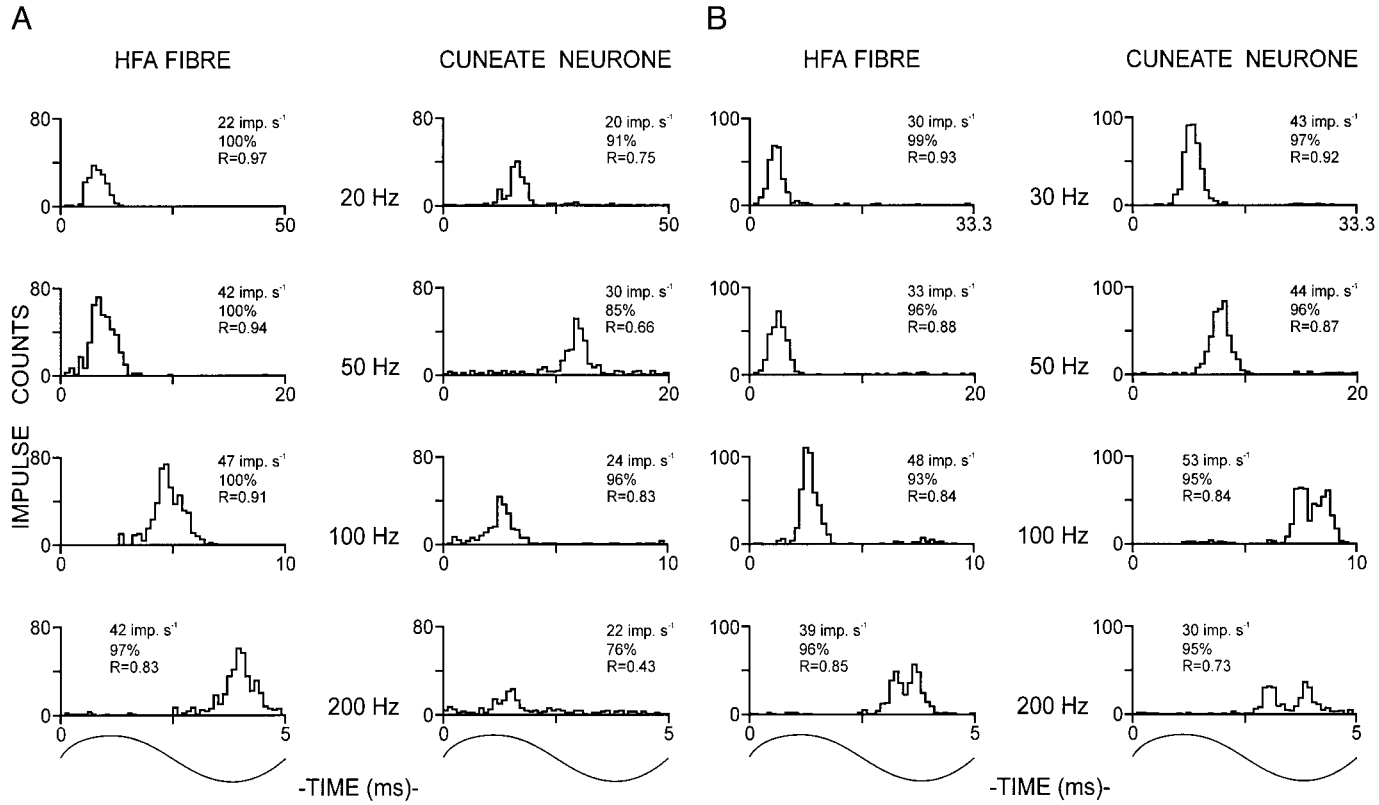

FIG. 8. Temporal patterning retained in the transmission of vibrotactile signals across the 1:1 synaptic linkage between single HFA fibers and cuneate neurons. Cycle histogram (CH) pairs show the probability of impulse occurrence within the vibration cycle period for the responses of 2 HFA fiber–cuneate neuron pairs (in *A* and *B*) at 4 different vibration frequencies (20–200 Hz in *A*, and 30–200 Hz in *B*). From the CHs, 2 quantitative measures of phase locking were derived. These were the percentage entrainment, which gave the highest percentage of impulses contained within any continuous half-cycle period of the vibration waveform (range of values: 50–100%), and the vector strength or the resultant (*R*), which provided an index of the phase coherence in the impulse distribution that is inversely related to the dispersion in the impulse occurrences around the mean phase of the response (range of values: 0–1). The impulse counts s^{-1}, percentage entrainment (%), and the resultant (*R*) are shown on the *right-hand side* of each histogram.

DISCUSSION

Identification of HFA-related cuneate neurons

The present study establishes that single HFA fibers have the capacity to drive central neurons of the cuneate nucleus. These fibers, representing one of the major classes of tactile sensory nerve fibers in the hairy skin, are readily distinguished on both functional properties and receptive field characteristics from the slowly adapting (SA) type I and II classes of tactile afferent that also innervate the hairy skin. First, the HFA fibers display a pure dynamic sensitivity to tactile stimuli, whereas the SAI and SAII afferents display maintained responses to static skin displacements (Chambers et al. 1972; Gynther et al. 1992, 1995; Iggo and Muir 1969; Vickery et al. 1992, 1994). Furthermore, the tactile sensitivity of SAI afferent fibers is associated with the small epidermal specializations, the ~200-μm-diam touch domes that are visible under the dissecting microscope in the shaved hairy skin (Iggo and Muir 1969), while that of SAII fibers is characterized by a responsiveness to static as well as dynamic components of skin stretch (Chambers et al. 1972; Gynther et al. 1992).

As the cuneate neurons driven by single HFA fibers had rostrocaudal, mediolateral, and depth locations consistent with the cluster zone of the nucleus (Hand and Van Winkle 1977), it is probable that they were cuneo-thalamic projection neurons as most neurons sampled electrophysiologically in this region can be activated antidromically from the contralateral thalamus (Andersen et al. 1964; Gordon and Jukes 1964). As the central recording was concentrated in this region of the nucleus, we cannot exclude the possibility that HFAs may also form potent connections with cuneate neurons outside the cluster zone. Although our analysis does not reveal the proportion of HFA fibers that have the capacity to drive cuneate neurons, the isolation of 21 pairs in which single HFA fibers were capable of activating cuneate neurons suggests that this potent form of synaptic linkage for the HFA fibers cannot be rare.

Security of the HFA-cuneate synaptic linkage

Previous studies have shown that the HFA class of tactile afferent fibers project via the dorsal columns to the cuneate and gracile divisions of the dorsal column nuclei and that HFA information is represented in the lemniscal output from the nuclei (Brown et al. 1974; Golovchinsky 1980; Gordon and Jukes 1964). However, the present study provides the first direct evidence that single HFA fibers can exert potent excitatory actions on their cuneate target neurons, and that the minimum sensory input conveyed over one of these sensory axons, a single impulse, can generate spike output from cuneate neurons. These observations on the 21 pairs therefore establish indirectly that unitary EPSPs generated by individual HFA fibers in their cuneate target neurons may be suprathresh-

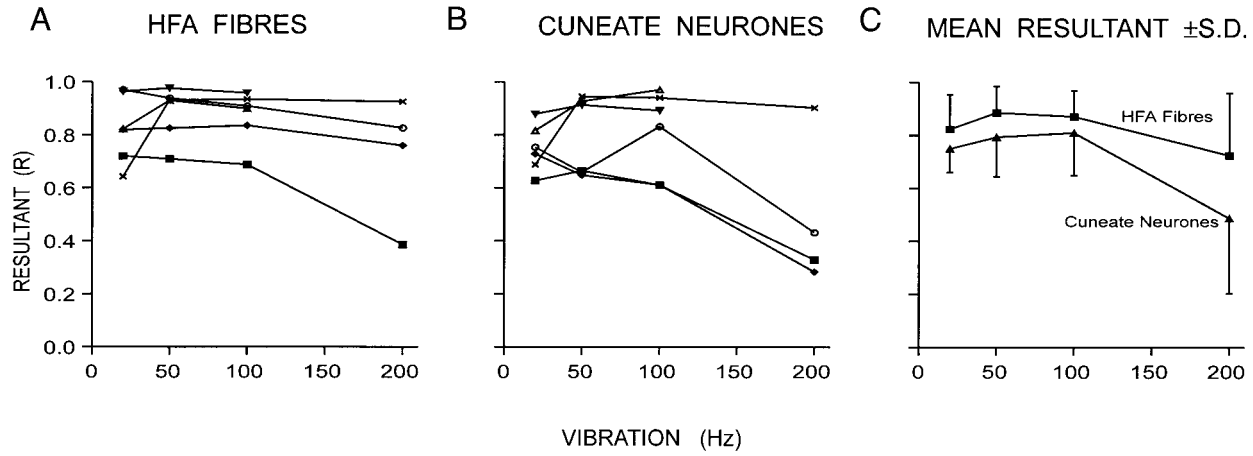

FIG. 9. Quantitative evaluation of changes in the phase locking of vibrotactile responses associated with transmission across the synaptic linkage formed by single HFA fiber–cuneate neuron pairs. The resultant (*R*), derived from cycle histogram distributions, is plotted as a function of vibration frequency in *A–C* as a measure of the tightness of phase locking for 6 individual HFA fibers (*A*) and their respective recorded cuneate target neurons (*B*). The mean *R* values (±SD) derived from *A* and *B* for the pre- and postsynaptic elements are plotted in *C*.

old. Furthermore, the paired analysis demonstrates that substantial amplification of the HFA input signal may occur, as the individual HFA spikes often give rise to a closely spaced burst of impulses consisting of either a spike doublet (Figs. 2, 3*A*, and 4) or multiple spike burst (Fig. 3*B*) from the cuneate neuron. This amplification could be sustained for perhaps the first 10–20 impulses arriving over the HFA fiber (Figs. 2, 4, and 6), in particular at rates up to 50 imp/s of HFA input, and may serve to enhance the probability of detecting weak tactile input signals. Furthermore, the spike bursts constituting the amplified response across this first synaptic junction in the dorsal column–lemniscal pathway may provide for a form of temporal summation to ensure secure transmission at the next synaptic junction, in the ventralposterior thalamic nucleus. These properties for the linkage between single HFA fibers and cuneate neurons suggest that transmission is optimized for the detection of minimal tactile sensory inputs arising in the HFA input channels.

We have not investigated in this study the extent of divergent and convergent actions on cuneate neurons by HFA afferents. However, as our earlier paired recording study of the transmission characteristics for individual PC-related afferent fibers revealed that individual PC fibers could activate multiple target neurons (Ferrington et al. 1986), we might expect that this form of amplification may also operate for HFA afferent fibers.

Vibrotactile signaling across the synaptic linkage between single HFA fibers and cuneate neurons

In the vibrotactile-induced responses of the HFA fiber-cuneate neuron pairs, it is also clear that this linkage is able to retain a temporally patterned sequence of spike activity in the cuneate neuron that reflects the periodicity of the vibration stimulus. This is apparent in the paired impulse trace records of Fig. 2, at 20 Hz, and in Figs. 4 and 7 at frequencies up to 100 Hz. Furthermore, even when the cuneate neuron was unable to respond on every cycle of the vibration stimulus the impulse activity remains phase locked at frequencies up to at least 200 Hz (Fig. 9). Although the tightness of phase locking, quantified in terms of the vector strength or *R* value calculated from the cycle histogram distributions, shows a statistically significant decline in the process of synaptic transmission from HFA fiber to cuneate neuron (Fig. 9*C*) this decline was small, and no more than about 10% at vibration frequencies up to 100 Hz. As the neural code for the frequency parameter of vibrotactile stimuli appears to depend on an impulse patterning that reflects the vibration periodicity (Ferrington and Rowe 1980b; Mountcastle et al. 1969; Talbot et al. 1968), it appears from paired HFA-cuneate response traces (Figs. 2 and 4) that in the process of synaptic transmission the cuneate neuron retains reliable information about the frequency parameter even in response to a selective input from a single HFA sensory fiber. At least this appears to be the case for the single HFA-cuneate linkage at vibration frequencies up to ~100 Hz. However, the vibration-induced impulse rates generated in the cuneate neurons by single HFA fibers were usually ≤100 imp/s, which are somewhat lower than those generated by vibration when the input is carried by single PC fibers (Ferrington et al. 1987a) or single SAI or SAII fibers (Gynther et al. 1995; Vickery et al. 1994). This difference appears to be attributable, in large part, to the more limited vibratory responsiveness of the HFA fibers themselves compared with the PC, SAI, and SAII fibers, each of which may be driven by focal vibration to rates of several hundred impulses/second (Ferrington et al. 1987a; Gynther et al. 1995; Vickery et al. 1994). Thus any limitation on the signaling of vibrotactile information by cuneate neurons activated from hairy skin may reflect limitations in the peripheral vibrotactile sensitivity of the HFA endings rather than deficiencies in transmission efficacy at the HFA-cuneate synaptic linkage. These constraints on peripheral HFA sensitivity probably account for the higher subjective vibrotactile thresholds in hairy skin compared with those in glabrous skin (Merzenich and Harrington 1969; Talbot et al. 1968; Verrillo 1966) and may also mean that the capacity for vibrotactile frequency discrimination in the hairy skin is poorer than in the glabrous skin. However, actual Weber fraction ($\Delta f/f$) data for this discrimination task are available only for glabrous skin (Goff 1967) or the sparsely haired skin of the anterior forearm (Rothenburg et al. 1977).

High transmission security at the dorsal column nuclei and the capacity of single tactile afferent fibers to contribute to perceptual experience

The high synaptic security revealed in the present study for the linkage between single HFA afferent fibers and cuneate neurons is similar to that shown in our previous studies for individual tactile afferent fibers of the PC, SAI, and SAII classes (Ferrington et al. 1987a,b; Gynther et al. 1995; Vickery et al. 1994). For all four classes, single fiber inputs are able to drive central neurons of the dorsal column nuclei with amplification of the input and reliable retention of temporal precision in the transmission of information about dynamic vibrotactile stimuli. As the HFA afferent fibers have now been shown to share these transmission attributes, it appears increasingly certain that high transmission security is a general attribute for different tactile sensory nerve classes at the dorsal column nuclei. To generate spike output from the postsynaptic neurons of this relay, there is no dependence on the elaborate spatial or temporal integrative processing that is required at the group Ia–motoneuron synaptic linkage. Instead, the transmission characteristics for tactile inputs at the dorsal column nuclei appear optimally designed for a sensing system, as reflected in its capacity to transmit signals about tactile perturbations that generate the minimal sensory input, a single afferent action potential.

Despite the high security of HFA fiber synaptic linkages with cuneate neurons, it remains uncertain whether the activation of individual HFA fibers can generate a tactile percept as this class of tactile fiber has not been tested for this capacity with the intraneural microstimulation procedure. When this microneurography technique has been used to selectively activate single tactile afferent fibers of other classes in conscious human subjects, it has revealed marked differences among these classes (Macefield et al. 1990; Ochoa and Torebjörk 1983; Vallbo et al. 1984). For example, the activation of single PC and RA fibers, and most SAI fibers, elicits a perceptual response, but the activation of single SAII fibers fails to do so. Furthermore, the activation of single SAI fibers with a train of electrical stimuli at 20–100 Hz elicits a subjective sense of steady skin pressure, but fails to generate any flutter-vibration percept in contrast to PC and RA fibers when activated in this way. However, despite these limitations for SAI and SAII fibers, the paired simultaneous recording analysis in the cat of transmission characteristics reveals a security and temporal precision of signaling for single SAI and SAII fibers that matches that for single PC afferent fibers (Ferrington et al. 1987a,b; Gynther et al. 1995; Vickery et al. 1994). Our original hypothesis, that the differential capacity of these fiber classes to contribute to perception when activated singly with the microneurography procedure, may be attributable to differential transmission characteristics at the dorsal column nuclei is therefore not born out by the results. Thus the explanation (unless there were some marked species difference between cat and man in this respect) must presumably be at higher levels of the sensory pathway, or be attributable to a more restricted central divergence and therefore a failure of individual SAI or SAII fibers to activate the necessary *critical mass* of central neurons for perceptual recognition. In view of these considerations, the high security of synaptic transmission for HFA fibers at the cuneate nucleus cannot be taken as evidence of their capacity for generating a perceptual response if activated singly.

High security for HFA linkages in parallel ascending sensory pathways

The HFA fibers, like most group II tactile afferent classes, project not just to the dorsal column nuclei but also to the dorsal horn, where they are known to be linked to neurons of the spinocervical tract (SCT) (Brown 1981; Brown and Noble 1982; Brown et al. 1986). The SCT neurons ascend ipsilaterally and synapse on neurons of the lateral cervical nucleus, which then have a crossed projection, joining the medial lemniscal outflow from the dorsal column nuclei (Brown 1981). HFA inputs are therefore known to project over at least two major parallel ascending tactile pathways. In their linkage with the SCT neurons of the dorsal horn, single HFA fibers can generate complex mono- and polysynaptic EPSPs, which, in some cases, lead to spike output in the target neuron (Brown et al. 1987a–c; Hongo and Koike 1975). Furthermore, the spike output may arise in burst form, indicative of amplification at this dorsal horn synapse. Thus the present results and the earlier observations at the dorsal horn indicate that single HFA fibers have potent excitatory synaptic linkages to at least two parallel ascending sensory systems. However, whether the temporal precision of impulse patterning present in the HFA responses to vibrotactile stimuli can be retained across the dorsal horn synaptic junction with SCT neurons is uncertain. The evidence from the study by Brown et al. (1987c) suggests that this may not be the case as the complex EPSPs evoked by single HFA input spikes are protracted, leading to a temporal dispersion in the spike output over a period of 10–15 ms (see Figs. 9 and 10 in Brown et al. 1987c). This temporal dispersion is far greater than the 2–3 ms observed for the spike bursts generated in cuneate neurons by single HFA input spikes (see Figs. 3 and 4 in present paper) and would presumably mean first, that phase locking of responses to vibrotactile stimuli in SCT neurons would be considerably poorer than the levels displayed by cuneate neurons, and second, that the capacity of the HFA fiber–SCT neuron linkage to convey information about the frequency parameter of vibrotactile disturbances in a temporal pattern code would be poorer than that of the HFA fiber–cuneate neuron linkages.

We acknowledge the technical assistance of C. Riordan and D. Sarno.

This work was supported by the National Health and Medical Research Council of Australia and the Australian Research Council.

REFERENCES

ANDERSEN P, ECCLES JC, SCHMIDT RF, AND YOKOTA T. Identification of relay cells and interneurons in the cuneate nucleus. *J Neurophysiol* 27: 1080–1095, 1964.

BLEDSOE SC, RUPERT AL, AND MOUSHEGIAN G. Response characteristics of cochlear nucleus neurons to 500 Hz tones and noise: findings relating to frequency-following potentials. *J Neurophysiol* 47: 113–127, 1982.

BROWN AG. Cutaneous afferent fibre collaterals in the dorsal columns of the cat. *Exp Brain Res* 5: 293–305, 1968.

BROWN AG. The spinocervical tract. *Prog Neurobiol* 17: 59–96, 1981.

BROWN AG, GORDON G, AND KAY RH. A study of single axons in the cat's medial lemniscus. *J Physiol (Lond)* 236: 225–246, 1974.

BROWN AG AND IGGO A. A quantitative study of cutaneous receptors and afferent fibres in the cat and rabbit. *J Physiol (Lond)* 193: 707–733, 1967.

BROWN AG, KOERBER HR, AND NOBLE R. Excitatory actions of single impulses in single hair follicle afferent fibres on spinocervical tract neurones in the cat. *J Physiol (Lond)* 382: 291–312, 1987a.

BROWN AG, KOERBER HR, AND NOBLE R. Actions of trains and pairs of impulses from single primary afferent fibres on single spinocervical tract cells in cat. *J Physiol (Lond)* 382: 313–329, 1987b.

BROWN AG, KOERBER HR, AND NOBLE R. An intracellular study of spinocervical tract cell responses to natural stimuli and single hair afferent fibres in cats. *J Physiol (Lond)* 382: 331–354, 1987c.

BROWN AG AND NOBLE R. Connexions between hair follicle afferent fibres and spinocervical tract neurones in the cat: the synthesis of receptive fields. *J Physiol (Lond)* 323: 77–91, 1982.

BROWN AG, NOBLE R, AND ROWE MJ. Receptive field profiles and integrative properties of spinocervical tract cells in the cat. *J Physiol (Lond)* 374: 335–347, 1986.

BURGESS PR, PETIT D, AND WARREN RM. Receptor types in cat hairy skin supplied by myelinated fibres. *J Neurophysiol* 31: 833–848, 1968.

CHAMBERS MR, ANDRES KH, DUERING MV, AND IGGO A. The structure and function of the slowly adapting type II mechanoreceptor in hairy skin. *Q J Exp Physiol* 57: 417–445, 1972.

FERRINGTON DG, HORA MOH, AND ROWE MJ. Functional maturation of tactile sensory fibers in the kitten. *J Neurophysiol* 52: 74–85, 1984.

FERRINGTON DG AND ROWE MJ. Functional capacities of tactile afferent fibres in neonatal kittens. *J Physiol (Lond)* 307: 335–353, 1980a.

FERRINGTON DG AND ROWE MJ. Differential contributions to coding of cutaneous vibratory information by cortical somatosensory areas I and II. *J Neurophysiol* 43: 310–331, 1980b.

FERRINGTON DG, ROWE MJ, AND TARVIN RPC. High gain transmission of single impulses through dorsal column nuclei of the cat. *Neurosci Lett* 65: 277–282, 1986.

FERRINGTON DG, ROWE MJ, AND TARVIN RPC. Action of single sensory fibres on cat dorsal column nuclei neurones: vibratory signalling in a one-to-one linkage. *J Physiol (Lond)* 386: 293–309, 1987a.

FERRINGTON DG, ROWE MJ, AND TARVIN RPC. Integrative processing of vibratory information in cat dorsal column nuclei neurones driven by identified sensory fibres. *J Physiol (Lond)* 386: 311–331, 1987b.

GOFF GD. Differential discrimination of frequency of cutaneous mechanical vibration. *J Exp Psychol* 74: 294–299, 1967.

GORDON G AND JUKES MGM. Dual organization of the exteroceptive components of the cat's gracile nucleus. *J Physiol (Lond)* 173: 263–290, 1964.

GOLOVCHINSKY V. Patterns of responses of neurons in cuneate nucleus to controlled mechanical stimulation of cutaneous velocity receptors in cat. *J Neurophysiol* 43: 1673–1699, 1980.

GREENSTEIN J, KAVANAGH P, AND ROWE MJ. Phase coherence in vibration-induced responses of tactile fibres associated with Pacinian corpuscle receptors in the cat. *J Physiol (Lond)* 386: 263–275, 1987.

GYNTHER BD, VICKERY RM, AND ROWE MJ. Responses of slowly adapting type II afferent fibres in cat hairy skin to vibrotactile stimuli. *J Physiol (Lond)* 458: 151–169, 1992.

GYNTHER BD, VICKERY RM, AND ROWE MJ. Transmission characteristics for the 1:1 linkage between slowly adapting type II fibers and their cuneate target neurons in cat. *Exp Brain Res* 105: 67–75, 1995.

HAND PJ AND VAN WINKLE T. The efferent connections of the feline nucleus cuneatus. *J Comp Neurol* 171: 83–109, 1977.

HONGO T AND KOIKE H. Some aspects of synaptic organization in the spinocervical tract cell in the cat. In: *The Somatosensory System*, edited by Kornhuber HH. Stuttgart, Germany: Thieme, 1975, p. 218–226.

IGGO A AND MUIR AR. The structure and function of a slowly adapting touch corpuscle in hairy skin. *J Physiol (Lond)* 200: 763–796, 1969.

IGGO A AND OGAWA H. Correlative physiological and morphological studies of rapidly adapting mechanoreceptors in cat's glabrous skin. *J Physiol (Lond)* 266: 275–296, 1977.

JÄNIG W. Morphology of rapidly and slowly adapting mechanoreceptors in the hairless skin of the cat's hind foot. *Brain Res* 28: 217–231, 1971.

JÄNIG W, SCHMIDT RF, AND ZIMMERMANN M. Single unit responses and the total afferent outflow from the cat's footpad upon mechanical stimulation. *Exp Brain Res* 6: 100–115, 1968.

LAVINE RA. Phase-locking in response of single neurons in cochlear nuclear complex of the cat to low-frequency tonal stimuli. *J Neurophysiol* 34: 467–483, 1971.

MACEFIELD G, GANDEVIA SC, AND BURKE D. Perceptual responses to microstimulation of single afferents innervating joints, muscles and skin of the human hand. *J Physiol (Lond)* 429: 113–129, 1990.

MACKIE PD, MORLEY JW, AND ROWE MJ. Signalling of static and dynamic features of muscle spindle input by external cuneate neurones in the cat. *J Physiol (Lond)* 519: 559–569, 1999.

MACKIE PD, MORLEY JW, ZHANG HQ, MURRAY GM, AND ROWE MJ. Signalling of static and dynamic features of muscle spindle input by cuneate neurones in the cat. *J Physiol (Lond)* 510: 923–939, 1998.

MARDIA KV. *Statistics of Directional Data.* London: Academic, 1972.

MERZENICH MM AND HARRINGTON T. The sense of flutter vibration evoked by stimulation on the hairy skin of primates: comparison of human sensory capacity with the responses of mechanoreceptor afferents innervating the hairy skin of monkeys. *Exp Brain Res* 9: 236–269, 1969.

MOUNTCASTLE VB, TALBOT WH, SAKATA H, AND HYVÄRINEN J. Cortical neuronal mechanisms in flutter vibration studied in un-anesthetized monkeys. Neuronal periodicity and frequency discrimination. *J Neurophysiol* 32: 452–484, 1969.

OCHOA J AND TOREBJÖRK E. Sensations evoked by intraneural microstimulation of single mechanoreceptor units innervating the human hand. *J Physiol (Lond)* 342: 633–654, 1983.

ROTHENBURG M, VERRILLO RT, ZAHORIAN SA, BRACHMAN ML, AND BOLANOWSKI SJ JR. Vibrotactile frequency for encoding a speech parameter. *J Acoust Soc Am* 62: 1003–1012, 1977.

TALBOT WH, DARIAN-SMITH I, KORNHUBER HH, AND MOUNTCASTLE VB. The sense of flutter-vibration: comparison of the human capacity with response patterns of mechano-receptive afferents from the monkey hand. *J Neurophysiol* 31: 301–334, 1968.

TUCKETT RP, HORCH KW, AND BURGESS PR. Response of cutaneous hair and field mechanoreceptors in cat to threshold stimuli. *J Neurophysiol* 41: 138–149, 1978.

VALLBO ÅB, OLSSON KÅ, WESTBERG K-G, AND CLARK FJ. Microstimulation of single tactile afferents from the human hand. Sensory attributes related to unit type and properties of receptive field. *Brain* 107: 727–747, 1984.

VERRILLO RT. Vibrotactile thresholds for hairy skin. *J Exp Psychol* 72: 47–50, 1966.

VICKERY RM, GYNTHER BD, AND ROWE MJ. Vibrotactile sensitivity of slowly adapting type I sensory fibres associated with touch domes in cat hairy skin. *J Physiol (Lond)* 453: 609–626, 1992.

VICKERY RM, GYNTHER BD, AND ROWE MJ. Synaptic transmission between single slowly adapting type I fibres and their cuneate target neurones in cat. *J Physiol (Lond)* 474: 379–392, 1994.

WINTER DL. N. gracilis of cat. Functional organization and corticofugal effects. *J Neurophysiol* 28: 48–70, 1965.

ZACHARIAH MK, ZHANG HQ, COLEMAN GT, AND ROWE MJ. Processing of input from single tactile afferent fibres associated with hair follicles by cuneate central neurones. *Proc Aust Neurosci Soc* 10: 174, 1999a.

ZACHARIAH MK, ZHANG HQ, COLEMAN GT, AND ROWE MJ. Amplification in the transmission of weak tactile signals across the cuneate synaptic relay. *Proc Aust Physiol Pharm Soc* 30: 141P, 1999b.

ZAR JH. *Biostatistical Analysis* (2nd ed.). Englewood Cliffs, NJ: Prentice-Hall, 1984.

ZHANG HQ, MURRAY GM, TURMAN AB, MACKIE PD, COLEMAN GT, AND ROWE MJ. Parallel processing of tactile information in the cerebral cortex of the marmoset monkey: effect of reversible inactivation of SI on the responsiveness of SII neurons. *J Neurophysiol* 76: 3633–3655, 1996.